Understanding the Properties of Donor-Acceptor Substituted Boron Difluoride 3-Cyanoformazanate Dyes

Francis L. Buguis,[a] Paul D. Boyle,[a] and Joe B. Gilroy*[a]

π-Conjugated materials offer attractive traits including semi-conductivity, low-energy light absorption/photoluminescence, and solution processability that render them ubiquitous within the organic electronics field. Among many strategies for property tuning, the creation of asymmetric electronic structures through the installation of donor and acceptor substituents commonly results in low-energy absorption/photoluminescence bands. Boron difluoride formazanate dyes are readily synthesized, can be asymmetrically substituted with donor and acceptor groups, and have unexpectedly low-energy absorption/photoluminescence bands that extend into the near-infrared. In this study, we prepared a series of donor-acceptor substituted boron difluoride 3-cyanoformazanate dyes and compared their properties to symmetric analogues. Our findings suggest that donor-acceptor derivatives are highly delocalized with properties intermediate of their symmetric counterparts. Furthermore, the data obtained suggest that the N-aryl substituents act as donors to the strongly accepting boron difluoride formazanate core, regardless of the functional groups appended to them. These properties were reproduced computationally, and while the frontier orbitals calculated for donor-acceptor dyes were modestly asymmetric, there was no evidence of charge-transfer character. This work provides significant insight into the unexpected properties of boron difluoride formazanates and reveals that their strongly accepting nature circumvents the predicted augmentation of electronic structure commonly observed for donor-accepter substituted dyes.

1. Introduction

Donor-acceptor (D-A) π-conjugated molecular and polymeric systems represent a growing class of materials that have received significant attention due to their structural modularity and unique electronic and photophysical properties.[1] Conjugated systems, specifically dyes, that contain D and A groups are typically designed to adopt a D-A or D-A-D electronic structure, and have been used for applications such as bioimaging and theranostics,[2] light-emitting materials,[3] and as reaction probes.[4] Systems that adopt an A-D-A electronic structure have also recently been recognized for their utility as organic semiconductors (OSC) due to their enhanced photostability for organic photovoltaics (OPV),[5] and light-emitting[6] applications. In contrast, dyes with D-A-A' electronic structures are relatively under-explored compared to their symmetric counterparts, specifically D-A-D and A-D-A motifs. Using the D-A-A' motif for OPVs leads t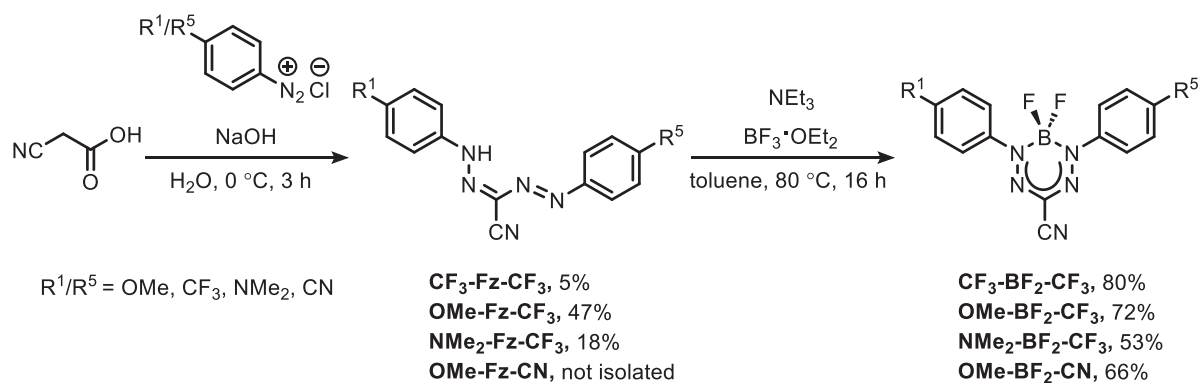o enhanced chargeseparation and suppression of electron-hole recombination which makes them excellent candidates for further exploration.[7] As such, significant efforts have been invested to understand structure-property relationships in existing dyes that adopt the D-A-A' motif.[8] Furthermore, the subtle interplay of donor and acceptor groups in D-D'-A'-A materials has strong implications on their nonlinear optical properties.[9]

Boron difluoride formazanates are an emerging class of dyes that boast accessible syntheses and tunable photophysical properties.[10] Research into these dyes demonstrates their feasibility for applications in areas such as photothermal therapy,[11] bioimaging,[12] OPVs,[13] and as triplet-sensitizers.[14] Thus far, structure-property studies have been limited to boron difluoride formazanate dyes that adopt D-A-D and A'-A-A' electronic structures due to their synthetic accessibility, whereby the boron difluoride formazanate core is the central chromophore (A), and the donor (D) and acceptor (A') are the substituents on the N-aryl rings.[15] In a bid to shift the absorbance and photoluminescence bands to the near-IR region, extension of π-conjugation and substitution with strongly donating groups like tertiary amines has been explored.[16] The interest in uncovering the molecular origins of the electrochemical and photophysical properties of boron difluoride formazanate dyes through experimentation and theoretical calculations is evident in the literature given that small π-conjugated molecules such as these dyes are not expected to yield the far red and near-IR photophysical properties desired and in current use for biological imaging applications.[17] To this end, we report boron difluoride 3-cyanoformazanate dyes that, on paper, possess D-A-A' electronic structures and compare the observed experimental properties to their D-A-D and A'-A-A' analogues in an effort to further red-shift their absorption and emission maxima and fully

[a] F. L. Buguis, P. D. Boyle, J. B. Gilroy
Department of Chemistry, The University of Western Ontario, 1151 Richmond St. N, London, Ontario N6A 5B7, Canada
E-mail: joe.gilroy@uwo.ca

Chem. Eur. J. **2025**, *31*, e202500675 (1 of 9)

© 2025 The Author(s). Chemistry – A European Journal published by Wiley-VCH GmbH

Chemistry–A European Journal

Research Article
doi.org/10.1002/chem.202500675

Chemistry Europe
European Chemical
Societies Publishing

Scheme 1. Synthesis of the title 3-cyanoformazan and their corresponding BF$_2$ formazanate dyes.

understand the origin of their highly unexpected photophysical properties.

2. Results and Discussion

2.1. Synthesis

In describing the structures of the compounds reported in this study, we adopted two conventions as short forms. The first, **R^1-Fz-R^5** describes 3-cyanoformazans where R^1 and R^5 are the substituents of the N-aryl rings and "Fz" describes the 3-cyanoformazanate core. Similarly, **R^1-BF$_2$-R^5** describes the boron difluoride formazanate dyes and "BF$_2$" represents the boron difluoride formazanate core. Examples of asymmetrically substituted boron difluoride formazanate dyes have been reported,[15b,c,18] but this is the first systematic study of electronic structure reported to date. To access 3-cyanoformazans bearing the same R^1 and R^5 substituents, we used 2 equiv. of the corresponding diazonium salt ([R-C$_6$H$_4$-N$_2$][Cl]), produced in situ. The syntheses of the 3-cyanoformazans required for this study were achieved by coupling aryldiazonium chloride salts with cyanoacetic acid under basic conditions (Scheme 1). The asymmetric formazans were synthesized similarly, using 1 equiv. of each corresponding diazonium chloride salt. The syntheses of the target formazans were characterized by a dramatic color change of the reaction mixture, from colorless to dark orange. After purification using column chromatography, diagnostic NH proton resonances (δ: 12.05–13.01) were observed in the respective ^{1}H NMR spectra (Figures S1–S6). The symmetrical formazan **CF$_3$-Fz-CF$_3$** was isolated from the reaction mixture used to prepare the asymmetric derivative **OMe-Fz-CF$_3$**. We attribute the low yield of the asymmetric formazan **NMe$_2$-Fz-CF$_3$** (18%) to the relative instability of the NMe$_2$-substituted aryldiazonium chloride salt, as evidenced by the persistent formation of an intractable foam. The boron difluoride formazanate adducts were synthesized by treating the 3-cyanoformazan precursors with excess NEt$_3$ and BF$_3$·OEt$_2$ (Scheme 1) to produce the respective dyes in 53–80% yields. The loss of the diagnostic NH resonance in the corresponding ^{1}H NMR spectra, along with the appearance of triplet and quartet signals in the ^{11}B and ^{19}F NMR spectra (Figures S7–S14) of the same compounds, indicated the successful transformation to the

corresponding boron difluoride formazanate. The furnished dyes were observed to be stable to aqueous work-up and purification via silica gel column chromatography. In addition, solutions in CDCl$_3$ left in ambient conditions were found to be stable for several weeks when monitored using ^{1}H NMR spectroscopy. Despite our best efforts, we were unable to isolate **OMe-Fz-CN** in pure form. However, its conversion to **OMe-BF$_2$-CN** proceeded in the same straightforward manner as the other boron difluoride formazanate dyes reported in this study. We also attempted the synthesis of the analogous formazan **NMe$_2$-Fz-CN**, but numerous attempts using a variety of reaction conditions did not lead to isolable amounts of the desired product. We attributed this to the instability of both the CN- and NMe$_2$-substituted diazonium chloride salts. Aryldiazonium chloride salts are known to have poor stability.[19] The spontaneous generation of dinitrogen entropically favors their decomposition and leads to the formation of a carbocation that is stabilized by strongly electron-donating groups. This stabilizing effect is more pronounced for amine-substituted aryldiazonium species, including Me$_2$N-ArN$_2^+$. In the case of CN-substituted arylamines, the strongly electron-withdrawing nature imparted by the -CN group led to slower conversion to the target aryldiazonium species. Consequently, there are competing factors that affect formation of the desired diazonium salt - specifically, the slow formation of the diazonium salt requires longer reaction times that, in turn, result in decomposition of the same diazonium salt as it is formed. We found that decomposition of CN-substituted aryldiazonium chloride interfered with the isolation of **OMe-Fz-CN** in pure form, thus, we opted for reaction conditions that produced replicable yields. We previously demonstrated the utility of [ArN$_2$][BF$_4$] salts in this context,[16d] however, those protocols were not deemed adaptable to the current library of compounds due to potential chemical incompatibility (i.e., the required combination of n-BuLi and CF$_3$/CN groups). The symmetric compounds **H-BF$_2$-H**, **OMe-BF$_2$-OMe**, **CN-BF$_2$-CN**, and **NMe$_2$-BF$_2$-NMe$_2$** were synthesized according to reported procedures.[15a,16d]

2.2. Solid-State Structures

Crystals of several boron difluoride formazanate dyes suitable for X-ray diffraction studies were studied to investigate their solid-state structures (Figure 1 and Table 1). The solid-state
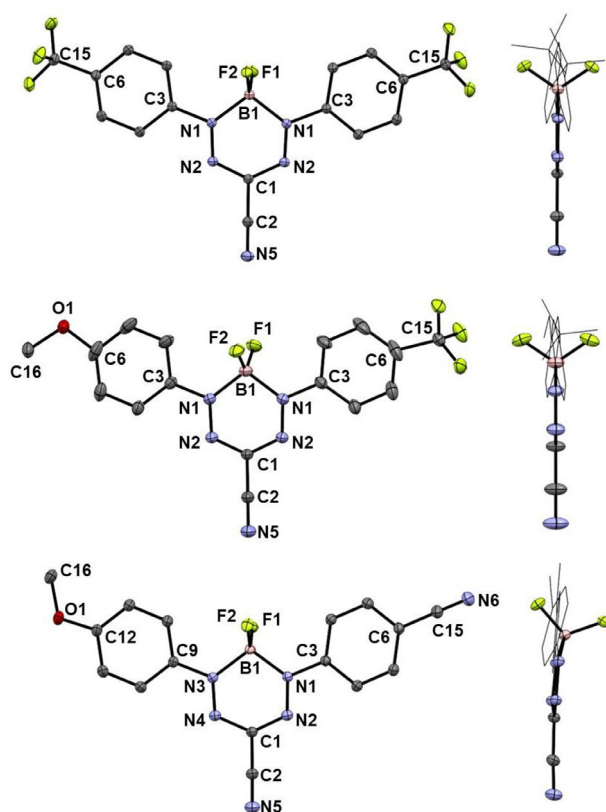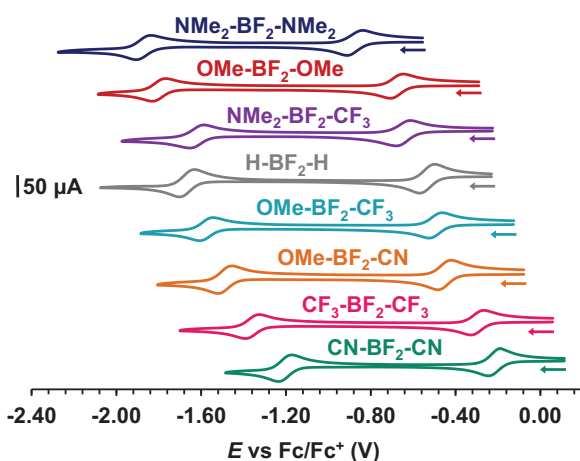
Figure 1. Top (left) and side (right) views of the solid-state structures of boron difluoride formazanate dyes **CF₃-BF₂-CF₃**, **OMe-BF₂-CF₃**, and **OMe-BF₂-CN**. Atomic displacement ellipsoids are shown at 50% probability. The hydrogen atoms are omitted, and the aryl rings are shown as wireframe structures for clarity.

structures for **CF₃-BF₂-CF₃** and **OMe-BF₂-CF₃** both crystallize in space group *C2/c* where the molecule straddles a crystallographic twofold axis which passes through atoms B1, C1, C5, and N5. This induces a 50:50 disorder in the **OMe-BF₂-CF₃** structure. In addition, for these structures both sides of the formazanate rings are symmetric with regard to their molecular geometries. In contrast, the **OMe-BF₂-CN** crystallizes in space group *P1̄* with the molecule residing on a general position in the unit cell. Analysis of the solid-state structures of these dyes revealed that the bond lengths within the formazanate core are intermediate of single and double bonds of the respective atoms. Structures that adopted a D-A-D motif have longer N1-N2/N3-N4 bond lengths, such as in **OMe-BF₂-OMe** [1.304(2) –1.307(2) Å] and **NMe₂-BF₂-NMe₂** [1.3134(14) – 1.3143(14) Å], than those that adopt an A′-A-A′ motif, such as in **CF₃-BF₂-CF₃** [1.2949(8) Å] and **CN-BF₂-CN** [1.2945(15) – 1.3017(15) Å]. The respective bond lengths observed for the structures that adopt the D-A-A′ motif, such as **OMe-BF₂-CF₃** [1.2994(10) Å] and **OMe-BF₂-CN** [1.2900(8) – 1.3115(8) Å] were not statistically different from those observed for their symmetric analogues. However, we do note that the N1-N2 bond length [1.3115(8) Å] are statistically different than the N3-N4 bond length [1.2900(8) Å] in **OMe-BF₂-CN**. The N1-C3/N3-C9 bond lengths are more sensitive to the substituent at the *para*-position. When compared to a typical $N_{(sp^3)}$-$C_{(Ar)}$ bond length (~1.425 Å),[20] the contracted N1-C2/N3-C9 bonds observed in **NMe₂-BF₂-NMe₂** [1.4140(16) – 1.4143(16) Å][16d] point to the presence of quinoidal character, while the same bonds were observed to be relatively long for **CF₃-BF₂-CF₃** (1.4331(8) Å) suggesting that that strongly electron-donating substituents at the N-aryl rings give rise to quinoidal character and significantly red-shifted photophysical

Table 1. Selected bond lengths, angles, and structural metrics for the title boron difluoride formazanate dyes. Additional structural refinement data for **OMe-BF₂-CF₃**, **CF₃-BF₂-CF₃**, and **OMe-BF₂-CN** are reported in Table S1.

Bond lengths (Å)	H-BF₂-H[15a]	OMe-BF₂-OMe[15a]	OMe-BF₂-CF₃	CF₃-BF₂-CF₃	NMe₂-BF₂-NMe₂[16c]	OMe-BF₂-CN	CN-BF₂-CN[15a]
N1 — N2	1.2900(15)	1.307(2)	1.2994(10)	1.2949(8)	1.3134(14)	1.3115(8)	1.3017(15)
N3 — N4	1.2948(15)	1.304(2)	-	-	1.3143(14)	1.2900(8)	1.2945(15)
N2 — C1	1.3408(17)	1.340(3)	1.3384(9)	1.3368(7)	1.3315(16)	1.3259(9)	1.3289(17)
N4 — C1	1.3379(17)	1.335(3)	-	-	1.3356(17)	1.3542(10)	1.3382(17)
N1 — C3	1.4344(16)	1.427(3)	1.4260(11)	1.4331(8)	1.4143(16)	1.4247(9)	1.4311(17)
N3 — C9	1.4306(17)	1.429(3)	-	-	1.4140(16)	1.4195(10)	1.4360(17)
N1 — B1	1.5748(18)	1.558(3)	1.5765(11)	1.5815(8)	1.5670(17)	1.5625(10)	1.5714(18)
N3 — B1	1.5771(17)	1.567(3)	-	-	1.5703(17)	1.5866(10)	1.5817(18)
Bond angles (°)							
N2 — N1 — B1	124.78(10)	124.39(18)	124.64(6)	124.68(5)	124.35(10)	124.21(5)	125.23(10)
N4 — N3 — B1	124.32(11)	124.17(17)	-	-	123.83(10)	123.64(6)	124.63(10)
N2 — C1 — N4	129.33(12)	130.0(2)	129.60(10)[c]	129.04(7)[c]	130.32(11)	129.63(6)	129.41(11)
N1 — B1 — N3	105.55(10)	106.85(17)	106.28(9)[c]	105.80(7)[c]	106.71(10)	106.45(5)	105.65(10)
Boron displacement (Å)[a]	0.192	0.143	0.00	0.00	0.136	0.172	0.025
Twist angle α_1 (°)[b]	26.16	21.80	10.10	11.21	18.51	17.09	17.06
Twist angle α_2 (°)[b]	18.70	15.72	10.10	11.21	18.74	1.08	4.65

[a] Distance between the boron and the plane defined by the N₄ atoms of the formazanate backbone.
[b] Angles between the planes defined by the *N*-aryl substituents and the N₄ atoms of the formazanate backbone.
[c] Although the nitrogen atoms at the 1/3 and 2/4 positions are crystallographically equivalent, the N2-C1-N4 and N1-B1-N3 labels are used for ease of comparison.

Chemistry–A European Journal

Research Article
doi.org/10.1002/chem.202500675

Chemistry
Europe
European Chemical
Societies Publishing

Figure 2. Cyclic voltammograms recorded for dry and degassed 0.1 mM solutions of boron difluoride formazanate dyes in CH_3CN containing 0.1 M $[nBu_4N][PF_6]$ as the supporting electrolyte at a scan rate of 250 mV s^{-1}. The arrows denote the initial scan direction.

Table 2. Cyclic voltammetry data recorded for solutions of the reported boron difluoride formazanate dyes in CH_3CN. Data were referenced internally to the ferrocene/ferrocenium redox couple.

	E_{red2} [V]	E_{red1} [V]	E_{ox} [V]
NMe$_2$-BF$_2$-NMe$_2$[16d]	–1.99	–1.03	0.25
OMe-BF$_2$-OMe[15a]	–1.80	–0.68	–
NMe$_2$-BF$_2$-CF$_3$	–1.62	–0.64	0.68
H-BF$_2$-H[15a]	–1.68	–0.53	–
OMe-BF$_2$-CF$_3$	–1.58	–0.49	–
OMe-BF$_2$-CN	–1.39	–0.45	–
CF$_3$-BF$_2$-CF$_3$	–1.36	–0.29	–
CN-BF$_2$-CN[15a]	–1.20	–0.26	–

properties. The trends in the experimental (X-ray) and theoretical (DFT) bond lengths for **NMe$_2$-BF$_2$-NMe$_2$** and **CF$_3$-BF$_2$-CF$_3$** (Table S2) were consistent, further suggesting that the degree of electronic communication between the formazanate core and the N-aryl rings is particularly dependent on the identity of the *para*-substituent at the N-aryl rings. Despite our best efforts, we were not able to grow crystals of **NMe$_2$-BF$_2$-CF$_3$** that were suitable for analysis.

2.3. Cyclic Voltammetry

The redox behavior of the synthesized compounds was studied using cyclic voltammetry experiments for solutions in acetonitrile (Figure 2 and Table 2). In all cases, we observed two reversible one-electron reduction events within the stability window of CH_3CN. The model compound **H-BF$_2$-H** served as a benchmark for the data we collected, which exhibited reduction events at $E_{red1} = -0.53$ V and $E_{red2} = -1.68$ V. The inclusion of electron-donating substituents shifted these reduction events to more negative potentials, as observed in the symmetrical dyes **OMe-BF$_2$-OMe** ($E_{red1} = -0.68$ V, $E_{red2} = -1.80$ V)[15a] and

NMe$_2$-BF$_2$-NMe$_2$ ($E_{red1} = -1.03$ V, $E_{red2} = -1.99$ V).[16d] Conversely, electron-withdrawing substituents led to a shift to less negative reduction potentials, as observed in the **CF$_3$-BF$_2$-CF$_3$** ($E_{red1} = -0.29$ V, $E_{red2} = -1.36$ V) and **CN-BF$_2$-CN** ($E_{red1} = -0.26$ V, $E_{red2} = -1.20$ V) dyes. The reduction events observed for the asymmetric compounds **OMe-BF$_2$-CF$_3$** ($E_{red1} = -0.49$ V, $E_{red2} = -1.58$ V), **NMe$_2$-BF$_2$-CF$_3$** ($E_{red1} = -0.64$ V, $E_{red2} = -1.62$ V), and **OMe-BF$_2$-CN** ($E_{red1} = -0.45$ V, $E_{red2} = -1.39$ V) were positioned between their respective symmetric analogues. One reversible one-electron oxidation event for **NMe$_2$-BF$_2$-CF$_3$** ($E_{ox} = 0.68$ V) and **NMe$_2$-BF$_2$-NMe$_2$** ($E_{ox} = 0.25$ V)[16d] associated with the aryl amine groups was also observed. These observations point to the strong electronic delocalization across the whole dye structure, which was responsive to the strength of electron donicity of the substituents at the *para*-position of the N-aryl rings.

2.4. Absorption and Photoluminescence Spectroscopy

Absorption and photoluminescence (PL) spectroscopy experiments showed that the identity of the substituent at the *para*-position of the N-aryl rings could be used to tune the photophysical properties of these dyes, with D-A-D derivatives proving to exhibit the lowest energy bands. Our discussion is limited to the photophysical properties observed for solutions in toluene, but the general trend followed suit for solutions in CH_2Cl_2, THF, and CH_3CN (Figure 3 and Table 3). Significant changes in the photophysical properties were not observed with respect to solvent polarity, suggesting that mechanisms involving chargetransfer were inoperative, including for D-A-A' compounds where charge transfer characteristics might be expected. Relative to our benchmark dye **H-BF$_2$-H**, which exhibited an absorption maximum (λ_{abs}) at 502 nm, the inclusion of EDGs, as in **OMe-BF$_2$-OMe** ($\lambda_{abs} = 572$ nm), shifted the absorption maxima to lower energies. We have previously reported that the inclusion of strongly electron-donating substituents, as in **NMe$_2$-BF$_2$-NMe$_2$** ($\lambda_{abs} = 728$ nm),[16c] effectively increases the extent of π-conjugation across the dye structure leading to near-IR photophysical properties.[16c,d] As such, amine-substituted boron difluoride formazanates have found use in applications such as photothermal theranostics and near-IR fluorescence imaging.,[10b,11,12c,21] The CF$_3$ groups, as in **CF$_3$-BF$_2$-CF$_3$** ($\lambda_{abs} = 498$ nm) shifted the absorption profile to higher energies relative to our benchmark. While CN substituents are strongly electron-withdrawing, the extension of π-conjugation led to a small shift to lower energies, as in **CN-BF$_2$-CN** ($\lambda_{abs} = 515$ nm).[15a] The compounds bearing both donor and acceptor substituents had absorption maxima intermediate of their symmetric analogues, as observed with **OMe-BF$_2$-CF$_3$** ($\lambda_{abs} = 554$ nm), **NMe$_2$-BF$_2$-CF$_3$** ($\lambda_{abs} = 668$ nm), and **OMe-BF$_2$-CN** ($\lambda_{abs} = 564$ nm). The wavelength of maximum PL (λ_{PL}) of these dyes followed the same trend as the λ_{abs} such that A'-A-A' ≈ **H-BF$_2$-H** < D-A-A' < D-A-D. The excitation spectra and excitation-PL matrices for selected compounds are shown in Figures S15–S19, demonstrating that maximum PL occurred when the excitation wavelength matched the respective λ_{abs}. PL lifetimes (τ in Table 3) were also measured for the model and title compounds (Table 3) in varying solvent polarities. In all cases, PL lifetimes
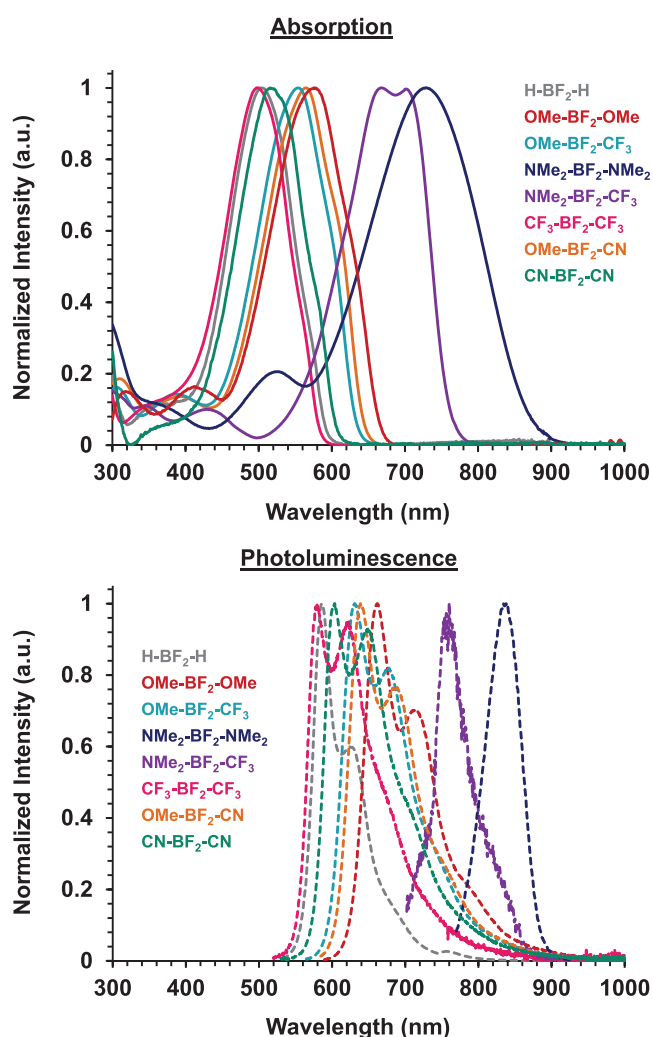
Chemistry–A European Journal

Research Article
doi.org/10.1002/chem.202500675

**Chemistry
Europe**
European Chemical
Societies Publishing

Absorption

Photoluminescence

Figure 3. Normalized UV-vis absorption and PL spectra of the reported boron difluoride formazanate dyes recorded for ~5 µM solutions in dry and degassed toluene.

were consistently longest for solutions in toluene and shortest for solutions in CH_3CN. We measured the PL quantum yield (Φ) of these compounds using the integrating sphere method. For the symmetrical dyes, we found that the inclusion of EDGs led to an increase in Φ relative to the model compound **H-BF$_2$-H**, while the inclusion of EWGs led to a decrease. The asymmetrical dyes **OMe-BF$_2$-CF$_3$** and **OMe-BF$_2$-CN** quantum yields intermediate of their respective symmetrical analogues. Interestingly, the dye **NMe$_2$-BF$_2$-CF$_3$** was measured to have the Φ = <1% in all solvents. We rationalize this observation with two reasons: i) The lower energy gap between the ground state and excited state promotes nonradiative decay according to the energy gap law.[22] and ii) this dye exhibited the narrowest Stokes shift (ν_{ST}) compared to the model and title dyes. This leads to a relatively larger spectral overlap, thus, a higher probability of reabsorption. Furthermore, we note that significant structural reorganization and nonemissive excited states have previously been implicated in the PL of boron difluoride formazanate dyes.[23]

2.5. DFT and TDDFT Studies

In order to rationalize our experimental results, we performed time-dependent density functional theory (TD-DFT) calculations at the M06/6–31+G* level of theory. Our theoretical calculations implicate the highest occupied molecular orbital (HOMO, π-type) and the lowest unoccupied molecular orbital (LUMO, π^*-type) as the orbital pair with the highest contribution to the absorption and PL maxima for each compound. The theoretical λ_{abs} and λ_{PL} were in good agreement with the experimental values (Table 3). The orbital isosurfaces extracted from the optimized ground- and excited-state geometries (Figures 4 and S20), respectively, revealed that the HOMOs and LUMOs were delocalized over the entire π-systems for boron difluoride formazanate dyes. Additionally, the frontier molecular orbitals had significant electronic density at the *para*-position of the N-aryl rings. The theoretical HOMO-LUMO gaps (E_g, Figure 5) followed the trend of our experimental results based on their structural motifs; A'-A-A' ≈ **H-BF$_2$-H** < D-A-A' < D-A-D. Notably, we observed modest asymmetry in the frontier orbital isosurfaces for asymmetric dyes **OMe-BF$_2$-CF$_3$**, **NMe$_2$-BF$_2$-CF$_3$**, and **OMe-BF$_2$-CN** with the HOMOs having greater contributions from the donor-substituted N-aryl rings and the LUMOs having greater contributions from the acceptor-substituted rings. However, there is significant overlap of the HOMO and LUMO isosurfaces at the boron difluoride formazanate core. Together with the results of our spectroscopic experiments, the properties discussed above point to the significant structure-property dependence of the formazanate core to the identity of the N-aryl rings. The highly electron-poor boron difluoride formazanate core appeared to render our asymmetric dyes immune from typical electronic structure considerations where D-A substituents are employed. They did not exhibit any significant charge-transfer characteristics, and their absorption/PL bands do not shift to lower energies than their symmetric analogues. Furthermore, although we introduced functional groups that would generally render the N-aryl substituents as electron donating or withdrawing, relative to the extremely electron poor boron difluoride formazanate core they appeared to all act as electron donors. Thus, based on conventional classifications of electron donating and withdrawing substituents, all existing boron difluoride formazanate dyes may be best described as having D-A-D electronic structures where the more strongly donating N-aryl substituents led to the lowest energy absorption and PL bands. These findings build on previous reports based on unrelated molecular architectures that demonstrated that strongly accepting substituents disrupt the nonlinear optical response of D-A polyenes.[24]

To further probe the electronic properties of the title compound, the dipole moments (µ) were obtained by performing TD-DFT calculations of the vertical electronic transitions at their optimized structure in the ground and excited states (Table 3). In general, the dipole moments at the ground state (µ$_{gs}$) were larger than the dipole moments at the excited state (µ$_{es}$), thus giving negative $\Delta\mu$. This was true for all solvents with varying solvent polarity. Asymmetrical dyes that adopt the D-A-A' motif were predicted to have larger µ$_{es}$ than µ$_{gs}$ (positive $\Delta\mu$),

Chem. Eur. J. **2025**, *31*, e202500675 (5 of 9)

© 2025 The Author(s). Chemistry – A European Journal published by Wiley-VCH GmbH

Chemistry–A European Journal

Research Article
doi.org/10.1002/chem.202500675

Chemistry Europe
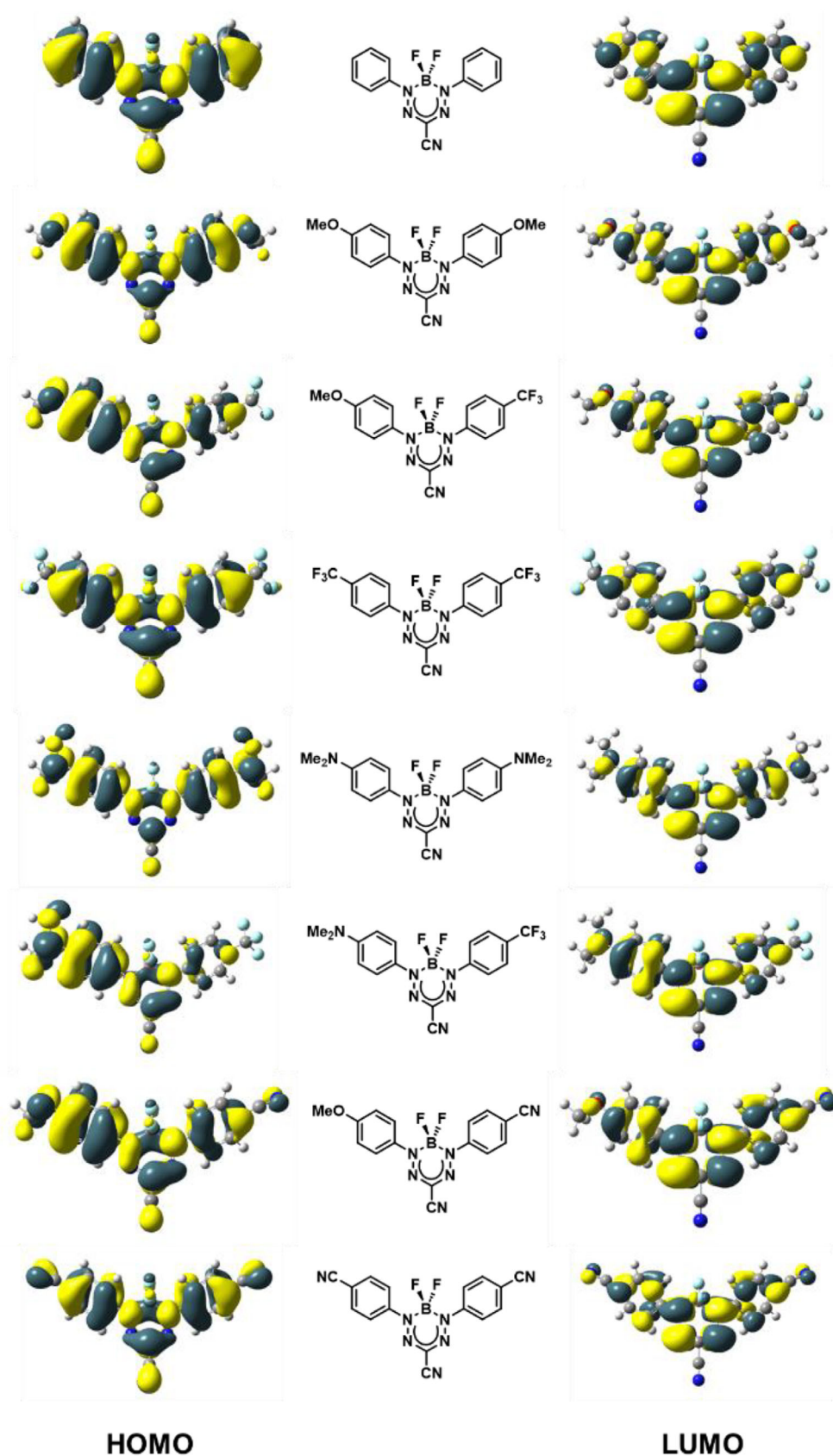European Chemical
Societies Publishing

Table 3. Experimental and calculated solution-state characterization data for the model and title boron difluoride formazanate dyes. The theoretical values were obtained using TDDFT with nonequilibrium solvation at the M06/6–31+G* SCRF = PCM level.

	Experiment							Theory				
	λ_{abs} [nm]	ε [M^{-1} cm^{-1}]	λ_{PL} [nm]	τ [ns]	$\Phi^{[a]}$ [%]	ν_{ST} [nm]	ν_{ST} [cm^{-1}]	λ_{abs} [nm]	λ_{PL} [nm]	μ_{gs} [D]	μ_{es} [D]	$\Delta\mu$ [D]
H-BF$_2$-H[15a]												
Toluene	502	30 400	586	2.2	3	84	2855	469	604	5.92	4.74	−1.18
CH$_2$Cl$_2$	492	34 600	584	0.1	2	93	3243	463	653	6.49	5.03	−1.46
THF	489	25 400	585	0.2	1	96	3356	462	649	6.44	5.07	−1.37
MeCN	479	24 700	582	0.1	1	103	3695	458	672	6.70	5.20	−1.50
OMe-BF$_2$-OMe[15a]												
Toluene	572	42 700	656	1.6	30	84	2239	537	670	6.60	3.35	−3.25
CH$_2$Cl$_2$	561	35 300	661	1.3	21	100	2697	536	653	7.40	3.54	−3.86
THF	559	33 400	662	1.2	18	103	2783	535	649	7.32	3.53	−3.79
MeCN	547	37 100	667	1.2	16	120	3289	532	668	7.73	3.58	−4.15
OMe-BF$_2$-CF$_3$												
Toluene	554	35 900	631	2.1	15	77	2203	516	635	7.97	8.45	0.48
CH$_2$Cl$_2$	542	34 200	631	0.9	13	89	2602	512	614	8.56	9.50	0.94
THF	539	34 200	635	0.6	7	96	2805	511	611	8.51	9.41	0.90
MeCN	524	33 300	636	0.1	1	112	3361	508	626	8.75	9.88	1.13
CF$_3$-BF$_2$-CF$_3$												
Toluene	498	27 500	579	1.1	2	81	2809	458	591	2.43	1.98	−0.45
CH$_2$Cl$_2$	485	28 600	570	0.1	1	85	3075	451	590	2.41	1.73	−0.68
THF	483	30 000	570	0.2	1	87	3160	451	588	2.41	1.73	−0.68
MeCN	473	33 500	563	0.2	<1	90	3380	447	600	2.46	1.74	−0.72
NMe$_2$-BF$_2$-CF$_3$												
Toluene	668	37 000	760	2.5	<1	84	1672	582	680	12.64	12.82	0.18
CH$_2$Cl$_2$	672	40 100	755	0.2	<1	83	1636	584	747	14.56	15.27	0.71
THF	678	41 100	768	0.8	<1	90	1728	583	740	14.40	15.06	0.66
MeCN	674	41 300	770	0.5	<1	96	1850	580	747	15.21	16.14	0.93
NMe$_2$-BF$_2$-NMe$_2$[16d]												
Toluene	728	41 300	834	4.6	7	106	1746	638	756	10.14	8.67	−1.47
CH$_2$Cl$_2$	733	41 300	866	0.1	4	133	2095	652	861	11.57	9.81	−1.76
THF	731	38 600	855	0.2	2	124	1984	649	851	11.44	9.71	−1.73
MeCN	728	43 600	888	0.3	<1	160	2475	651	908	12.09	10.23	−1.86
OMe-BF$_2$-CN												
Toluene	564	41 600	639	1.4	26	75	2081	526	645	9.42	10.48	1.06
CH$_2$Cl$_2$	554	38 400	639	1.1	14	85	2401	524	631	10.14	11.77	1.63
THF	548	41 000	643	0.6	8	95	2696	523	628	10.09	11.66	1.57
MeCN	534	45 400	642	0.1	1	108	3150	519	643	10.34	12.22	1.88
CN-BF$_2$-CN[15a]												
Toluene	515	35 800	598	2.5	3	83	2695	483	610	0.47	0.10	−0.37
CH$_2$Cl$_2$	499	33 700	589	0.2	2	90	3062	473	572	0.40	0.05	−0.35
THF	497	41 100	590	0.2	2	93	3172	473	571	0.41	0.03	−0.38
MeCN	473	35 900	591	0.1	1	118	4221	467	578	0.38	0.12	−0.26

[a] Determined using an integrating sphere.

suggesting that the excited state for these compounds was more polarized compared to symmetrical analogs. Dyes that adopted the A'-A-A' motif (i.e., CF$_3$-BF$_2$-CF$_3$ and CN-BF$_2$-CN) were also predicted to have the lowest μ values. Taken together, these theoretical findings were consistent with and corroborate the results

from experimental spectroscopy such that the optical properties of the title dyes do not depend significantly on solvent polarity. Furthermore, EWGs lead to more even distribution of electron deficiency, thereby lowering μ values, while EDGs introduce regimes of higher electron density (thus, higher μ values),

Chemistry–A European Journal

Research Article
doi.org/10.1002/chem.202500675

Chemistry Europe
European Chemical
Societies Publishing

HOMO   **LUMO**

Figure 4. Frontier molecular orbitals of the optimized ground-state structures of the model and title boron difluoride formazanate dyes calculated at the M06/6–31+G* level of theory.
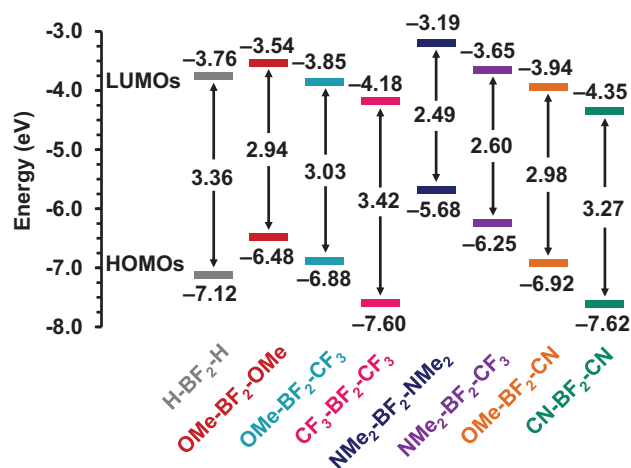
Chem. Eur. J. **2025**, *31*, e202500675 (7 of 9)

© 2025 The Author(s). Chemistry – A European Journal published by Wiley-VCH GmbH

Chemistry–A European Journal

Research Article
doi.org/10.1002/chem.202500675

**Chemistry
Europe**
European Chemical
Societies Publishing

Figure 5. Energies (eV) of the frontier molecular orbitals at the ground-state geometry of boron difluoride formazanate dyes calculated at the M06/6–31+G* level of theory with nonequilibrium solvation in toluene.

highlighting the electron-deficient nature of the formazanate core.

3. Conclusion

We report the synthesis and characterization of asymmetrically substituted boron difluoride 3-cyanoformazanate dyes that were suggested to have D-A-A' electronic structures and corroborate our experimental observations using theoretical computations. These dyes exhibited photophysical and electrochemical properties intermediate of their D-A-D and A'-A-A' analogues and notably did not benefit from charge-transfer characteristics that might be expected to lead to significantly red-shifted absorption and PL maxima. The molecular origins of the observed properties relate to the extremely electron-poor nature of the boron difluoride formazanate core, which, in essence, renders the N-aryl substituents as electron donors compared to the strongly accepting boron difluoride formazanate core, regardless of their *para*-substituents. Thus, the properties observed were primarily dictated by the boron difluoride formazanate core and the degree of electronic (resonance) delocalization associated with the N-aryl substituents, rather than charge-transfer arguments typical of D-A architectures.

This study enhances the understanding of the far-red and near-IR photophysical properties of boron difluoride formazanate dyes, which are completely unexpected for molecules with such small π-systems, and leads to the discovery of new derivatives which are of significant interest for bioimaging and theranostics development. Furthermore, this study suggests that D-A design strategies are not universal and that the nature of the central chromophore requires careful consideration. In this case, the boron difluoride formazanate core precludes access to charge-transfer characteristics and limits the efficacy of this design strategy. These considerations are likely applicable to other systems with strongly electron-poor or electron-rich cores and will inform the design of forthcoming materials within the field.

Acknowledgments

Conflict of Interests

The authors declare no conflict of interest.

Data Availability Statement

The data that support the findings of this study are available in the supplementary material of this article.

[1] a) S. Xu, Y. Duan, B. Liu, *Adv. Mater.* **2020**, *32*, 1903530; b) L. Li, X. Han, M. Wang, C. Li, T. Jia, X. Zhao, *Chem. Eng. J.* **2021**, *417*, 128844; c) D. Meng, R. Zheng, Y. Zhao, E. Zhang, L. Dou, Y. Yang, *Adv. Mater.* **2022**, *34*, 2107330; d) X. Chen, X. Zhang, X. Xiao, Z. Wang, J. Zhao, *Angew. Chem., Int. Ed.* **2023**, *62*, e202216010; e) M. Clerc, S. Sandlass, O. Rifaie-Graham, J. A. Peterson, N. Bruns, J. Read de Aaniz, L. F. Boesel, *Chem. Soc. Rev.* **2023**, *52*, 8245; f) L. Ding, Z.-D. Yu, X.-Y. Wang, Z.-F. Yao, Y. Lu, C.-Y. Yang, J.-Y. Wang, J. Pei, *Chem. Rev.* **2023**, *123*, 7421; g) Y. Yang, Y. Xie, F. Zhang, *Adv. Drug Delivery Rev.* **2023**, *193*, 114697.

[2] a) S. Zhu, R. Tian, A. L. Antaris, X. Chen, H. Dai, *Adv. Mater.* **2019**, *31*, 1900321; b) Z. Lei, F. Zhang, *Angew. Chem. Int. Ed.* **2021**, *60*, 16294; c) B. Lu, Y. Huang, Z. Zhang, H. Quan, Y. Yao, *Mater. Chem. Front.* **2022**, *6*, 2968.

[3] a) P. Ledwon, *Org. Electron.* **2019**, *75*, 105422; b) H. J. Kim, T. Yasuda, *Adv. Opt. Mater.* **2022**, *10*, 2201714; c) K. R. Naveen, R. K. Konidena, P. Keerthika, *Chem. Rec.* **2023**, *23*, e202300208; d) R. Wang, C.-S. Lee, Z. Lu, *J. Organomet. Chem.* **2023**, *984*, 122564.

[4] a) J. Wu, C. Shao, X. Ye, X. Di, D. Li, H. Zhao, B. Zhang, G. Chen, H.-K. Liu, Y. Qian, *ACS Sens.* **2021**, *6*, 863; b) X.-Y. Liu, X.-J. Wang, L. Shi, Y.-H. Liu, L. Wang, K. Li, Q. Bu, X.-B. Cen, X.-Q. Yu, *Anal. Chem.* **2022**, *94*, 7665; c) W.-C. Yang, S.-Y. Li, S. Ni, G. Liu, *Aggregate* **2024**, *5*, e460.

[5] a) C.-K. Wang, X. Che, Y.-C. Lo, Y.-Z. Li, Y.-H. Wang, S. R. Forrest, S.-W. Liu, K.-T. Wong, *Chem. Asian J.* **2020**, *15*, 2520; b) X. Wan, C. Li, M. Zhang, Y. Chen, *Chem. Soc. Rev.* **2020**, *49*, 2828; c) Y. Chen, Y. Zheng, Y. Jiang, H. Fan, X. Zhu, *J. Am. Chem. Soc.* **2021**, *143*, 4281; d) J. Wang, P. Xue, Y. Jiang, Y. Huo, X. Zhan, *Nat. Rev. Chem.* **2022**, *6*, 614; e) G. Zhang, F. R. Lin, F. Qi, T. Heumüller, A. Distler, H.-J. Egelhaaf, N. Li, P. C. Y. Chow, C. J. Brabec, A. K. Y. Jen, H.-L. Yip, *Chem. Rev.* **2022**, *122*, 14180.

[6] C. P. Keshavananda Prabhu, K. R. Naveen, J. Hur, *Mater. Chem. Front.* **2024**, *8*, 769.

[7] a) S. P. Singh, M. S. Roy, A. Thomas, K. Bhanuprakash, G. D. Sharma, *Org. Electron.* **2012**, *13*, 3108; b) C.-H. Chen, H.-C. Ting, Y.-Z. Li, Y.-C. Lo, P.-H. Sher, J.-K. Wang, T.-L. Chiu, C.-F. Lin, I. S. Hsu, J.-H. Lee, S.-W. Liu, K.-T. Wong, *ACS Appl. Mater. Interfaces* **2019**, *11*, 8337; c) C.-H. Chen, C.-J. Chen, Y.-A. Chen, Y.-H. Chang, H.-C. Liu, Y.-C. Lo, B.-Y. Lin, C.-L. Lin, C. J. Easley, C. J. Bardeen, Y.-S. Chen, J.-H. Lee, T.-L. Chiu, K.-T. Wong, *Energy*

Chem. Eur. J. **2025**, *31*, e202500675 (8 of 9)

© 2025 The Author(s). Chemistry – A European Journal published by Wiley-VCH GmbH

Chemistry–A European Journal

Research Article
doi.org/10.1002/chem.202500675

Chemistry Europe
European Chemical
Societies Publishing

Fuels **2021**, *35*, 19024; d) M. G. Bekmez, N. Öztürk, B. S. Arslan, D. Avcı, M. Nebioğlu, İ. Şişman, *Dyes Pigm.* **2024**, *229*, 112317.

[8] a) Y. Sugihara, N. Inai, M. Taki, T. Baumgartner, R. Kawakami, T. Saitou, T. Imamura, T. Yanai, S. Yamaguchi, *Chem. Sci.* **2021**, *12*, 6333; b) J. Zhang, H. Li, B. Lin, X. Luo, P. Yin, T. Yi, B. Xue, X.-L. Zhang, H. Zhu, Z. Nie, *J. Am. Chem. Soc.* **2021**, *143*, 19317; c) X. Zhu, L. Feng, S. Cao, J. Wang, G. Niu, *Org. Lett.* **2022**, *24*, 8305; d) W. Ma, Z. Bin, G. Yang, J. Liu, J. You, *Angew. Chem. Int. Ed.* **2022**, *61*, e202116681; e) Y. Liu, J. Yang, Z. Mao, D. Ma, Y. Wang, J. Zhao, S.-J. Su, Z. Chi, *Adv. Opt. Mater.* **2023**, *11*, 2201695; f) S. Cao, X. Tian, M. Cao, J. Wang, G. Niu, B. Z. Tang, *Chem. Mater.* **2023**, *35*, 2472.

[9] a) P. R. Varanasi, A. K. Y. Jen, J. Chandrasekhar, I. N. N. Namboothiri, A. Rathna, *J. Am. Chem. Soc.* **1996**, *118*, 12443; b) I. D. L. Albert, T. J. Marks, M. A. Ratner, *J. Am. Chem. Soc.* **1997**, *119*, 6575; c) L. Beverina, J. Fu, A. Leclercq, E. Zojer, P. Pacher, S. Barlow, E. W. Van Stryland, D. J. Hagan, J.-L. Brédas, S. R. Marder, *J. Am. Chem. Soc.* **2005**, *127*, 7282.

[10] a) J. B. Gilroy, E. Otten, *Chem. Soc. Rev.* **2020**, *49*, 85; b) S. Yang, K. Lu, H. Xiao, *Curr. Opin. Chem. Biol.* **2024**, *81*, 102473.

[11] H. Xiang, L. Zhao, L. Yu, H. Chen, C. Wei, Y. Chen, Y. Zhao, *Nat. Commun.* **2021**, *12*, 218.

[12] a) R. R. Maar, S. M. Barbon, N. Sharma, H. Groom, L. G. Luyt, J. B. Gilroy, *Chem. - Eur. J.* **2015**, *21*, 15589; b) N. Sharma, S. M. Barbon, T. Lalonde, R. R. Maar, M. Milne, J. B. Gilroy, L. G. Luyt, *RSC Adv.* **2020**, *10*, 18970; c) S. Wang, H. Shi, L. Wang, A. Loredo, S. M. Bachilo, W. Wu, Z. Tian, Y. Chen, R. B. Weisman, X. Zhang, Z. Cheng, H. Xiao, *J. Am. Chem. Soc.* **2022**, *144*, 23668.

[13] J. D. B. Koenig, M. E. Farahat, J. S. Dhindsa, J. B. Gilroy, G. C. Welch, *Mater. Chem. Front.* **2020**, *4*, 1643.

[14] T. Khrootkaew, S. Wangngae, K. Chansaenpak, K. Rueantong, W. Wattanathana, P. Pinyou, P. Panajapo, V. Promarak, K. Sagarik, A. Kamkaew, *Chem. Asian J.* **2024**, *19*, e202300808.

[15] a) S. M. Barbon, P. A. Reinkeluers, J. T. Price, V. N. Staroverov, J. B. Gilroy, *Chem. Eur. J.* **2014**, *20*, 11340; b) S. M. Barbon, J. T. Price, P. A. Reinkeluers, J. B. Gilroy, *Inorg. Chem.* **2014**, *53*, 10585; c) M.-C. Chang, A. Chantzis, D. Jacquemin, E. Otten, *Dalton Trans.* **2016**, *45*, 9477; d) J. S. Dhindsa, F. L. Buguis, M. Anghel, J. B. Gilroy, *J. Org. Chem.* **2021**, *86*, 12064; e) F. L. Buguis, P. D. Boyle, J. B. Gilroy, *Dyes Pigm.* **2022**, *198*, 110002.

[16] a) S. M. Barbon, V. N. Staroverov, J. B. Gilroy, *J. Org. Chem.* **2015**, *80*, 5226; b) S. M. Barbon, J. T. Price, U. Yogarajah, J. B. Gilroy, *RSC Adv.* **2015**, *5*, 56316; c) R. R. Maar, R. Zhang, D. G. Stephens, Z. Ding, J. B. Gilroy, *Angew. Chem. Int. Ed.* **2019**, *58*, 1052; d) F. L. Buguis, R. R. Maar, V. N. Staroverov, J. B. Gilroy, *Chem. Eur. J.* **2021**, *27*, 2854.

[17] a) M.-C. Chang, E. Otten, *Inorg. Chem.* **2015**, *54*, 8656; b) A. D. Laurent, E. Otten, B. Le Guennic, D. Jacquemin, *J. Mol. Model.* **2016**, *22*, 263; c) C. Kumar, A. R. Agrawal, N. G. Ghosh, H. S. Karmakar, S. Das, N. R. Kumar, V. W. Banewar, S. S. Zade, *Dalton Trans.* **2020**, *49*, 13202; d) P. Suwannakham, P. Panajapo, P. Promma, T. Khrootkaew, A. Kamkaew, K. Sagarik, *RSC Adv.* **2024**, *14*, 20081.

[18] S. Novoa, J. B. Gilroy, *Polym. Chem.* **2017**, *8*, 5388.

[19] a) T. G. R. Ullrich, *Thermochim. Acta* **1993**, *225*, 201; b) T. Grewer, D. J. Frurip, B. K. Harrison, *J. Loss. Prev. Process Ind.* **1999**, *12*, 391; c) V. D. Filimonov, E. A. Krasnokutskaya, A. A. Bondarev, *Bondarev in Structures, Stability, and Safety of Diazonium Salts*, Eds.: M. M. Chehimi, J. Pinson, and F. Mousli), Springe Nature, **2022**, pp. 35–57; d) C. Bravo-Díaz, E. González-Romero, in *Kinetics and Mechanisms of Aryldiazonium Ions in Aqueous Solutions*, Eds.: M. M. Chehimi, J. Pinson, and F. Mousli), Springer Nature, **2022**, pp. 58–77; e) J. Mateos, T. Schulte, D. Behera, M. Leutzsch, A. Altun, T. Sato, F. Waldbach, A. Schnegg, F. Neese, T. Ritter, *Science* **2024**, *384*, 446.

[20] W. M. Haynes, D. R. Lide, T. J. Bruno, *CRC Handbook of Chemistry and Physics*, CRC Press, Boca Raton, Florida, **2016**, p. 337.

[21] M. Yang, S. Wang, X. Ou, J. Ni, S. Segawa, J. Sun, F. Xu, R. T. K. Kwok, J. Zhao, J. W. Y. Lam, G. Jin, B. Z. Tang, *ACS Nano* **2024**, *18*, 30069.

[22] a) R. Englman, J. Jortner, *Mol. Phys.* **1970**, *18*, 145; b) M. Bixon, J. Jortner, J. Cortes, H. Heitele, M. E. Michel-Beyerle, *J. Phys. Chem.* **1994**, *98*, 7289.

[23] A. Melenbacher, J. S. Dhindsa, J. B. Gilroy, M. J. Stillman, *Angew. Chem. Int. Ed.* **2019**, *58*, 15339.

[24] S. R. Marder, C. B. Gorman, B. G. Tiemann, L. T. Cheng, *J. Am. Chem. Soc.* **1993**, *115*, 3006.